Exotic Non-Abelian Topological Defects in Lattice Fractional Quantum Hall States

Zhao Liu,[1] Gunnar Möller,[2,3,*] and Emil J. Bergholtz[4]
[1]*Dahlem Center for Complex Quantum Systems and Institut für Theoretische Physik, Freie Universität Berlin, Arnimallee 14, 14195 Berlin, Germany*
[2]*Functional Materials Group, School of Physical Sciences, University of Kent, Canterbury CT2 7NZ, United Kingdom*
[3]*TCM Group, Cavendish Laboratory, University of Cambridge, Cambridge CB3 0HE, United Kingdom*
[4]*Department of Physics, Stockholm University, AlbaNova University Center, 106 91 Stockholm, Sweden*
(Received 9 March 2017; published 7 September 2017)

We investigate extrinsic wormholelike twist defects that effectively increase the genus of space in lattice versions of multicomponent fractional quantum Hall systems. Although the original band structure is distorted by these defects, leading to localized midgap states, we find that a new lowest flat band representing a higher genus system can be engineered by tuning local single-particle potentials. Remarkably, once local many-body interactions in this new band are switched on, we identify various Abelian and non-Abelian fractional quantum Hall states, whose ground-state degeneracy increases with the number of defects, i.e, with the genus of space. This sensitivity of topological degeneracy to defects provides a "proof of concept" demonstration that genons, predicted by topological field theory as exotic non-Abelian defects tied to a varying topology of space, do exist in realistic microscopic models. Specifically, our results indicate that genons could be created in the laboratory by combining the physics of artificial gauge fields in cold atom systems with already existing holographic beam shaping methods for creating twist defects.

DOI: 10.1103/PhysRevLett.119.106801

Introduction.—Extrinsic defects embedded in topologically ordered phases of matter [1–5] may acquire exotic properties [6–22]. Genons [11,12], named after their ability to effectively increase the genus of space thus enhancing the topological degeneracy, are particularly intriguing representatives of this idea and can be visualized as twist defects at the ends of branch cuts connecting separate "world sheets" of different components in the host system. Importantly, the linkage of genons to the topology of space and the underlying topological order establishes them as powerful tools to overcome the long-standing challenge of accessing topological orders on surfaces with tunable genus. It also imparts them with nontrivial quantum dimensions and braiding statistics that are significantly different from those of intrinsic quasiparticles of the host system [12], thus enabling fault tolerant topological quantum computation [23,24] even in Abelian host states without this capability and extending our knowledge of topological order. However, while the beautiful idea of genons is based on topological field theory [11,12] and corroborated by complicated exactly solvable models [6,10,16], its actual relevance to realistic microscopic models has remained open.

In this Letter, we fill this void by presenting the first evidence of genons in a microscopic lattice model which can favor lattice fractional quantum Hall states, i.e., fractional Chern insulators [25,26], and naturally host defects. With a scheme to offset the negative influence of defects on the band structure, we obtain compelling results that explicitly demonstrate the remarkable fingerprint of genons—the nontrivial dependence of the topological degeneracy on the number of defects which effectively tune the genus of space to high numbers. Our results provide a deep insight into the physical realization of genons in simple lattice models involving only single-particle hopping and on site two-body interactions, thus opening up the experimental accessibility of topological orders on high-genus surfaces.

Model.—We consider particles in a two-dimensional square lattice with two internal degrees of freedom (referred to as "layers" for convenience) $\sigma = \uparrow, \downarrow$ on each lattice site and an effective magnetic flux ϕ piercing each elementary plaquette (Fig. 1). We introduce $\mathbb{Z}_2$ twist defects [12] into the lattice such that a particle's layer index is flipped when it moves around such a defect once. It is helpful to imagine

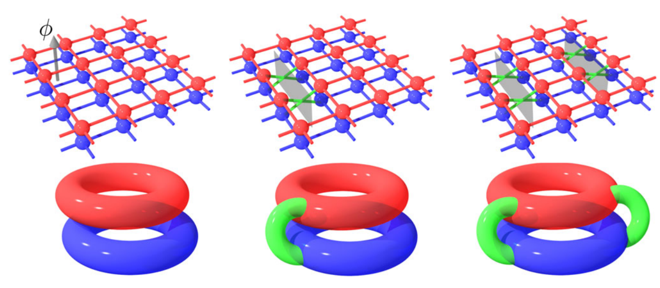

FIG. 1. Our model is equivalent to two square lattice layers (blue and red) where each plaquette is pierced by an effective flux ϕ (upper left panel). We only plot nearest-neighbor hopping for simplicity. Defects are introduced through branch cuts (transparent gray) where the particles switch layer (green). We study systems with up to two such branch cuts, corresponding to topologies resembling wormholes, as displayed in the bottom panels.

that the layer flipping occurs precisely when a particle hops across a branch cut that we take to connect a pair of defects in a straight line (Fig. 1). We thus formulate the tight-binding Hamiltonian as

$$H_0 = \sum_{j,k,\sigma} t(z_j, z_k) a^{\dagger}_{j,\mathcal{F}^{n_{jk}}(\sigma)} a_{k,\sigma}, \tag{1}$$

where $a^{\dagger}_{j,\sigma}$ ($a_{j,\sigma}$) creates (annihilates) a particle in layer σ at lattice site $z_j = x_j + iy_j$, and $\mathcal{F}^{n_{jk}}(\sigma)$ accounts for n_{jk} flips of the initial layer σ when a straight line from z_k to z_j intersects with n_{jk} branch cuts. The hopping coefficient from z_k to z_j is designed as $t(z_j, z_k) = (-1)^{x+y+xy} e^{-(\pi/2)(1-\phi)|z|^2} e^{-i\pi\phi(x_j+x_k)y}$ [27,28], where $z = z_j - z_k = x + iy$. Such a hopping is local in the sense that $t(z_j, z_k)$ follows a superexponential decay. We focus on $\phi = 1/q$ with integer q, for which a unit cell contains q sites in the x direction. Without defects, H_0 has a $\mathbb{Z}_2$ symmetry associated with exchanging two layers and corresponds to two decoupled Kapit-Mueller models [27] in the Landau gauge; thus, its lowest band contains two copies of an exactly flat band with Chern number $\mathcal{C} = 1$.

The effective topology of our model strongly depends on the number of branch cuts (Fig. 1). If each layer has a torus geometry, a branch cut plays the role of a wormhole connecting two tori [11]; hence, M branch cuts effectively lead to a single surface with genus $g = M + 1$. In the following, we arrange all branch cuts in the y direction without loss of generality [29], denoting the branch cut connecting a pair of defects at (X_1, Y_1) and (X_1, Y_2) as $(X_1, Y_1 \to Y_2)$ [35].

Single-particle spectra and defect-induced localized states.—We diagonalize H_0 on a periodic lattice $\mathcal{L}$ of $L_x \times L_y$ sites to analyze the effect of defects on the band structure [36]. Without defects, the lowest $2\phi L_x L_y$ single-particle levels are exactly degenerate at zero energy. This flatness is seriously distorted by M pairs of defects, and we identify $4M$ levels with a significant deviation from the original band structure: $2M$ of them (levels $\epsilon_1, \ldots, \epsilon_{2M}$) drop below the original lowest band, and another $2M$ ($\epsilon_{2\phi L_x L_y - M+1}, \ldots \epsilon_{2\phi L_x L_y + M}$) move into the original lowest band gap. Moreover, they form nearly degenerate clusters, respectively. An example of the band structure for $M = 1$ is shown in Fig. 2(a). We further examine the eigenvectors of these $4M$ levels. Remarkably, they are all strongly localized near the defects [Fig. 2(b)], and the localization becomes weaker or completely disappears for other levels with less deviation from the original band structure. This localization enables us to do a controlled tuning of the deviated energies by local potentials near the defects without significantly distorting the rest of the band structure, as we explain below.

Higher genus flat bands.—The effectively increased genus does not guarantee that defects in our model can be thought of as genons. We must show that topological

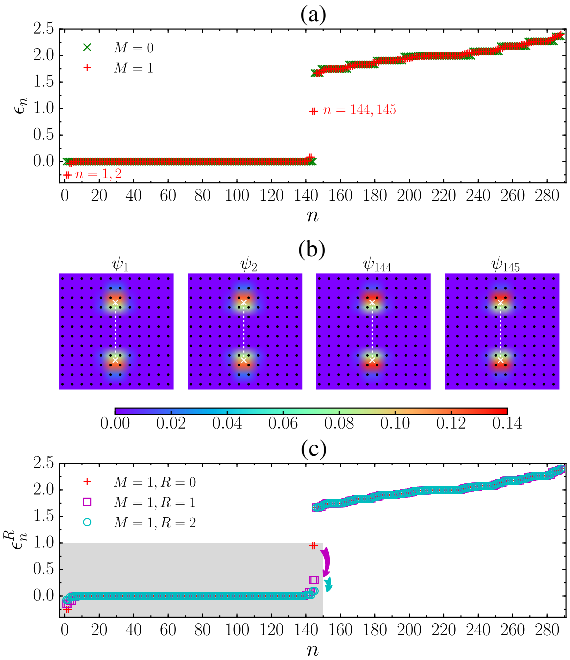

FIG. 2. Band structure for a $L_x \times L_y = 12 \times 12$ lattice with $\phi = 1/2$. (a) The spectrum $\{\epsilon_n\}$ of H_0. Without defects ($M = 0$), $\epsilon_1, \ldots, \epsilon_{144}$ are exactly degenerate at zero energy. With one branch cut [$M = 1$, white dashed line in (b)] at $(5.5, 2.5 \to 8.5)$, the original band structure is distorted, with two nearly degenerate clusters (ϵ_1, ϵ_2) and $(\epsilon_{144}, \epsilon_{145})$ having the largest deviation. (b) The lattice site weight of eigenvectors ψ_1, ψ_2, ψ_{144}, ψ_{145} of H_0 for the same defects as in (a). All of them are strongly localized near the defects. The eigenstates with less energy deviation from the original band structure, for example, ψ_3, ψ_4, ψ_{142}, ψ_{143}, are less localized (not shown here). (c) The spectrum $\{\epsilon_n^R\}$ of $H_0 + V$ with $R = 0$, 1, and 2 and the same defects as in (a). $\epsilon_1^R, \ldots, \epsilon_{145}^R$ which we must flatten (shaded in gray) becomes more degenerate for larger R, with the flatness $(\epsilon^R_{2\phi L_x L_y+M+1} - \epsilon^R_{2\phi L_x L_y+M})/(\epsilon^R_{2\phi L_x L_y+M} - \epsilon^R_1) \approx 0.6, 3.1, 9.4$ for $R = 0$, 1, 2.

phases can be stabilized on the high-genus surfaces created by these defects, and that they display defect-enhanced topological degeneracy. Tuning deviated single-particle energies to recover a flat lowest band is necessary for reaching this goal. We consider $N_b = (k/2)(2\phi L_x L_y)$ bosons interacting via $(k+1)$-body on site repulsions

$$H_{\mathrm{int}} = \sum_{i\in\mathcal{L},\sigma=\uparrow,\downarrow} {:}n_{i,\sigma} n_{i,\sigma} \cdots n_{i,\sigma}{:} \tag{2}$$

with integer $k \geq 1$ [37]. In this setup, the ground state without defects is two copies of model $\mathcal{Z}_k$ Read-Rezayi (RR) states on the lattice, residing in the lowest $2\phi L_x L_y$ exactly degenerate eigenstates of H_0 with filling fraction $\nu = N_b/(2\phi L_x L_y) = k/2$ [38,39]. Adding M pairs of defects effectively deforms the topology to a single $g = M + 1$ surface but should not change ν in the thermodynamic limit.

Hence, in that case the most promising candidate for the underlying topological phase is the $\mathcal{Z}_k$ RR state on a single $g = M + 1$ surface. In the continuum, such a state resides in N_s exactly degenerate single-particle states in the lowest Landau level, with

$$N_s = 2N_b/k - (1 - g), \tag{3}$$

where $\nu = \lim_{N_b\to\infty} N_b/N_s = k/2$, and the extra offset $1 - g$ is related to the topological "shift" [40,41]. Consequently, in our lattice model with M pairs of defects, Eq. (3) combined with $N_b = (k/2)(2\phi L_x L_y)$ and $g = M + 1$ requires a flat band consisting of the lowest $N_s = 2\phi L_x L_y + M$ single-particle eigenstates of H_0 to host the $\mathcal{Z}_k$ RR state. However, this set of eigenstates corresponds to a residual flat band plus all significantly deviated levels [Fig. 2(a)]. As the emergence of FQH liquids requires a hierarchy of energy scales such that interactions dominate the band dispersion of the low-energy band, we must first flatten this large band dispersion to amplify the interaction effect before a topological state can be realized. Fortunately, this can be readily achieved by local potentials owing to the strong localization of the deviated states near defects [Fig. 2(b)]. A simple candidate of such a local potential [29] is $V = -\sum_{n=1}^{2\phi L_x L_y + M} \epsilon_n \mathcal{T}_R(|\psi_n\rangle\langle\psi_n|)$, where ϵ_n's and ψ_n's are the eigenvalues and eigenvectors of H_0, respectively, and $\mathcal{T}_R$ denotes the truncation at a radius R around each defect. The dominant terms in V exactly correspond to the deviated levels, because others staying at $\epsilon_n = 0$ have no contributions. As expected, a very small R is already sufficient to do the flattening very well, with negligible influence on the pertinent eigenvector subspace. In Fig. 2(c), we show the band structure of $H_0 + V$ with $M = 1$ and $R = 0, 1, 2$, respectively. The degeneracy between the lowest $2\phi L_x L_y + M$ energy levels indeed becomes better with the increase of R, with the flatness significantly increased to ≈9.4 for $R = 2$. The corresponding eigenvectors of $H_0 + V$ have a total 99% overlap with those of H_0 for $R = 1$ and $R = 2$.

Defect-enhanced topological degeneracy.—After ensuring that a new lowest flat band can be recovered, we are now in the position to examine whether interactions can stabilize the $\mathcal{Z}_k$ RR states in the single high-genus surfaces created by defects, characterized by the defect-enhanced topological degeneracy $\mathcal{D}$ [42]. We project the interaction H_{int}, which is assumed to be small relative to the band gap, to the lowest $2\phi L_x L_y + M$ eigenstates of H_0 [43] and neglect their energy dispersion for large numerical efficiency. This procedure is similar to the band projection in the flat-band limit extensively used to study fractional Chern insulators without defects [33].

In the most realistic $k = 1$ case, we find compelling evidence that defects lead to a $\nu = 1/2$ Laughlin state on effective high-genus surfaces. Without defects, the ground state is two copies of $\nu = 1/2$ Laughlin states on the torus with $\mathcal{D} = 2 \times 2 = 4$. Although we still get $\mathcal{D} = 4$ with one pair of defects, consistent with the $\nu = 1/2$ Laughlin state on a single $g = 2$ surface, a nontrivial enhancement of $\mathcal{D}$ from 4 to 8 occurs for two pairs of defects ($g = 3$), characterized by eight approximately degenerate ground states for various system sizes [Fig. 3(a)]. These states are separated from other excited states by an energy gap which is significantly larger than the ground-state splitting, and the splitting is reduced relative to the gap as the system size—and thus the separation of defects—is increased. The eight ground states never mix with other excited states under twisted boundary conditions [28] [Fig. 3(b)], which confirms the robustness of topological degeneracy. In order to further corroborate their topological nature, we compute the particle entanglement spectra (PES) [33,44,45] to probe the quasihole excitation property. We find a clear gap in the PES, at the number of levels matching the corresponding counting of quasihole excitations [Fig. 3(c)] [29,33]. Our results unambiguously indicate that the ground state with M pairs of defects is the $\nu = 1/2$ Laughlin state on a single $g = M + 1$ surface with degeneracy $\mathcal{D}_M^{k=1} = 2^{M+1}$. While the inclusion of a local potential V is crucial for obtaining topological degeneracies, the specific choice thereof is less crucial for larger systems stemming from their topological origin [29].

The effect of defects is even more intriguing at higher k's with non-Abelian host states. For $k = 2$, the ground state in the absence of defects is two copies of Moore-Read (MR) states on the torus, with $\mathcal{D} = 9$ for even $N_b/2$ and $\mathcal{D} = 1$ for odd $N_b/2$. Strikingly, in this case, unlike the situation of

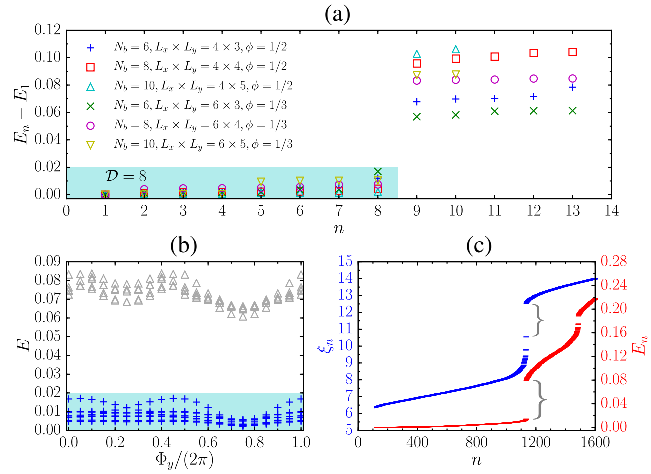

FIG. 3. Defect-enhanced topological degeneracy for Abelian systems at $\nu = 1/2$ with two branch cuts [35]. (a) The energy spectra of various system sizes. The eight quasidegenerate ground states are highlighted by the cyan shade. (b) The y-direction spectral flow for $N_b = 6$, $L_x \times L_y = 4 \times 3$, $\phi = 1/2$. The eight ground states (blue +) never mix with excited states (gray △). (c) The PES (blue) for $N_b = 8$, $L_x \times L_y = 6 \times 4$, $\phi = 1/3$ in the $N_b^A = 4$ sector and the corresponding quasihole excitations (red) for $N_b = 4$, $L_x \times L_y = 6 \times 4$, $\phi = 1/3$. The number of states below the gaps (indicated by the gray }) are identical in both spectra.

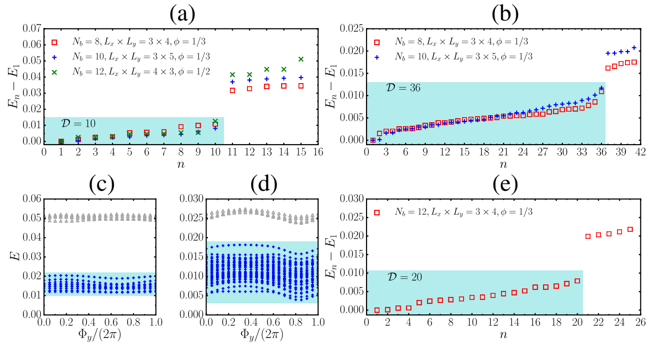

FIG. 4. Defect-enhanced topological degeneracy for non-Abelian systems. The approximately degenerate ground states, together with the degeneracy $\mathcal{D}$, are highlighted by the cyan shade. (a) The energy spectra at $\nu = 1$ with one pair of defects [35]. (b) The energy spectra at $\nu = 1$ with two pairs of defects [35]. (c) The y-direction spectral flow for $N_b = 10$, $L_x \times L_y = 3 \times 5$, $\phi = 1/3$ with the same branch cut as in (a). (d) The y-direction spectral flow for $N_b = 10$, $L_x \times L_y = 3 \times 5$, $\phi = 1/3$ with the same branch cuts as in (b). (e) The energy spectrum at $\nu = 3/2$ with one pair of defects [35].

$k = 1$, one pair of defects already leads to a nontrivial enhancement of $\mathcal{D}$ to 10 for all even N_b, which becomes better for larger system sizes and is robust under twisted boundary conditions [Figs. 4(a) and 4(c)]. By adding another pair of defects, $\mathcal{D}$ is further enhanced to 36 [Figs. 4(b) and 4(d)], with a faster growth rate than the $k = 1$ case. The dependence of the topological degeneracy on the number of defects convincingly suggests that, by introducing M pairs of defects for $k = 2$, the ground state evolves to the $\nu = 1$ MR state on a single $g = M + 1$ surface with degeneracy $\mathcal{D}_M^{k=2} = 2^M(2^{M+1} + 1)$ [46]. The enhancement of the topological degeneracy is also observed for $k = 3$, where $\mathcal{D}$ is increased from 16 to 20 by adding $M = 1$ pair of defects [Fig. 4(e)], consistent with the $\nu = 3/2$ $\mathcal{Z}_3$ RR state on a single $g = M + 1$ surface with degeneracy $\mathcal{D}_M^{k=3} = 2[(5 + \sqrt{5})^M + (5 - \sqrt{5})^M]$ [46].

The topological phases with defect-enhanced ground-state degeneracy strongly indicate that the defects in our model are indeed genons. In particular, each of them carries a distinct nontrivial quantum dimension $d = \lim_{M\to\infty}(\mathcal{D}_M)^{1/(2M)}$ from that of intrinsic quasiparticles of the host state. At $\nu = 1/2$, we have non-Abelian genons with $d = \sqrt{2}$, although the Laughlin state only has Abelian quasiparticles. More saliently, genons at $\nu = 1$ in our model have $d = 2$ thus allowing for universal quantum computation, while the quasiparticles of the MR state itself cannot [12,24]. At $\nu = 3/2$, we obtain genons with even higher quantum dimension $d = (5 + \sqrt{5})^{1/2}$. These differences, together with the projective braiding statistics of defects [12], open the possibility that genons are more powerful tools for topological quantum computation than ordinary quasiparticles.

Discussion.—In this work, we condense the beautiful idea of genons from topological field theory into a recipe for realistic microscopic lattice models. We identify a number of different lattice genons in both Abelian and non-Abelian host states based on their numerically observed defect-enhanced ground-state degeneracy, which can be thought of as adding genons into the system. The key ingredients of our proposal are already experimentally available and their combined synthesis is plausibly within reach—especially for coupled Laughlin states emerging from a particularly simple on site two-body interaction. Artificial gauge fields generated by lattice shaking techniques are compatible with multiple internal degrees of freedom as we require. The long-range hopping, which is chosen for theoretical elegance and numerical efficiency, is in fact not essential for the existence of lattice genons [29]. Hence, the already realized Hofstadter model in optical lattices [47,48] can serve as an eminently promising candidate platform for creating genons, while its higher Chern bands provide an additional variety of host quantum Hall liquids [34,49]. In particular, a recent realization [50] based on a quantum gas microscope already allows single-site addressing, and could be combined with holographic beam shaping methods [51] that provide a natural route towards producing the branch cuts and local potentials necessary to realize lattice genons as we envision. Furthermore, a time-dependent control over the locations of such branch cuts would enable braiding experiments that may directly probe their exchange statistics.

We thank N. R. Cooper and J. Behrmann for useful discussions. Z. L. was supported by an Alexander von Humboldt Research Fellowship for Postdoctoral Researchers and the U.S. Department of Energy, Office of Basic Energy Sciences through Grant No. DE-SC0002140. The latter was specifically for the use of computational facilities at Princeton University. G. M. is supported by The Royal Society, Grant No. UF120157, and acknowledges use of the Darwin Supercomputer of the University of Cambridge High Performance Computing Service, funded by Strategic Research Infrastructure Funding from the Higher Education Funding Council for England and funding from the Science and Technology Facilities Council. E. J. B. was supported by the Swedish research council (VR) and the Wallenberg Academy Fellows program of the Knut and Alice Wallenberg Foundation.

All three authors contributed equally to this work.

*Corresponding author.
G.Moller@kent.ac.uk

[1] R. B. Laughlin, Anomalous Quantum Hall Effect: An Incompressible Quantum Fluid with Fractionally Charged Excitations, Phys. Rev. Lett. 50, 1395 (1983).

[2] X. G. Wen, Topological orders and Chern-Simons theory in strongly correlated quantum liquid, Int. J. Mod. Phys. B **05**, 1641 (1991).

[3] G. Moore and N. Read, Nonabelions in the fractional quantum hall effect, Nucl. Phys. **B360**, 362 (1991).

[4] M. Oshikawa and T. Senthil, Fractionalization, Topological Order, and Quasiparticle Statistics, Phys. Rev. Lett. **96**, 060601 (2006).

[5] J. Maciejko and G. A. Fiete, Fractionalized topological insulators, Nat. Phys. **11**, 385 (2015).

[6] H. Bombin, Topological Order with a Twist: Ising Anyons from an Abelian Model, Phys. Rev. Lett. **105**, 030403 (2010).

[7] J. C. Y. Teo and C. L. Kane, Majorana Fermions and Non-Abelian Statistics in Three Dimensions, Phys. Rev. Lett. **104**, 046401 (2010).

[8] M. Freedman, M. B. Hastings, C. Nayak, X.-L. Qi, K. Walker, and Z. Wang, Projective ribbon permutation statistics: A remnant of non-Abelian braiding in higher dimensions, Phys. Rev. B **83**, 115132 (2011).

[9] N. H. Lindner, E. Berg, G. Refael, and A. Stern, Fractionalizing Majorana Fermions: Non-Abelian Statistics on the Edges of Abelian Quantum Hall States, Phys. Rev. X **2**, 041002 (2012).

[10] Y.-Z. You and X.-G. Wen, Projective non-Abelian statistics of dislocation defects in a Z_N rotor model, Phys. Rev. B **86**, 161107 (2012).

[11] M. Barkeshli and X.-L. Qi, Topological Nematic States and Non-Abelian Lattice Dislocations, Phys. Rev. X **2**, 031013 (2012).

[12] M. Barkeshli, C.-M. Jian, and X.-L. Qi, Twist defects and projective non-Abelian braiding statistics, Phys. Rev. B **87**, 045130 (2013).

[13] M. Barkeshli, C.-M. Jian, and X.-L. Qi, Theory of defects in Abelian topological states, Phys. Rev. B **88**, 235103 (2013).

[14] A. Vaezi, Fractional topological superconductor with fractionalized Majorana fermions, Phys. Rev. B **87**, 035132 (2013).

[15] Y.-Z. You, C.-Ming Jian, and X.-G. Wen, Synthetic non-Abelian statistics by Abelian anyon condensation, Phys. Rev. B **87**, 045106 (2013).

[16] B. J. Brown, S. D. Bartlett, A. C. Doherty, and S. D. Barrett, Topological Entanglement Entropy with a Twist, Phys. Rev. Lett. **111**, 220402 (2013).

[17] A. Vaezi, Superconducting Analogue of the Parafermion Fractional Quantum Hall States, Phys. Rev. X **4**, 031009 (2014).

[18] J. Fuchs and C. Schweigert, A note on permutation twist defects in topological bilayer phases, Lett. Math. Phys. **104**, 1385 (2014).

[19] M. Barkeshli, H.-C. Jiang, R. Thomale, and X.-L. Qi, Generalized Kitaev Models and Extrinsic Non-Abelian Twist Defects, Phys. Rev. Lett. **114**, 026401 (2015).

[20] H. Zheng, A. Dua, and L. Jiang, Demonstrating non-Abelian statistics of Majorana fermions using twist defects, Phys. Rev. B **92**, 245139 (2015).

[21] Y. You and Y.-Z. You, Geometry defects in bosonic symmetry-protected topological phases, Phys. Rev. B **93**, 245135 (2016).

[22] A. Bühler, N. Lang, C. V. Kraus, G. Möller, S. D. Huber, and H. P. Büchler, Majorana modes and p-wave superfluids for fermionic atoms in optical lattices, Nat. Commun. **5**, 4504 (2014).

[23] A. Y. Kitaev, Fault-tolerant quantum computation by anyons, Ann. Phys. (Amsterdam) **303**, 2 (2003).

[24] C. Nayak, S. H. Simon, A. Stern, M. Freedman, and S. Das Sarma, Non-Abelian anyons and topological quantum computation, Rev. Mod. Phys. **80**, 1083 (2008).

[25] S. A. Parameswaran, R. Roy, and S. L. Sondhi, Fractional quantum Hall physics in topological flat bands, C.R. Phys. **14**, 816 (2013).

[26] E. J. Bergholtz and Z. Liu, Topological flat band models and fractional Chern insulators, Int. J. Mod. Phys. B **27**, 1330017 (2013).

[27] E. Kapit and E. Mueller, Exact Parent Hamiltonian for the Quantum Hall States in a Optical Lattice, Phys. Rev. Lett. **105**, 215303 (2010).

[28] In a finite system with periodic boundary conditions, both the lattice sites and defects appear periodically. To adjust Eq. (1) to periodic boundary conditions, we replace $t(z_j, z_k)$ by $\sum_{s,t=-\infty}^{+\infty} t(z_j + sL_x + itL_y, z_k) e^{2\pi i s L_x y_j \phi}$, and in n_{jk} we count all crossings between the hopping from z_k to $z_j + sL_x + itL_y$ and the periodically appearing branch cuts. Twisted boundary conditions can be implemented by replacing $t(z_j, z_k)$ by $\sum_{s,t=-\infty}^{+\infty} t(z_j + sL_x + itL_y, z_k)$ $e^{2\pi i s L_x y_j \phi} e^{-is\Phi_x} e^{-it\Phi_y}$.

[29] See Supplemental Material at http://link.aps.org/supplemental/10.1103/PhysRevLett.119.106801 for short-range hopping tight-binding models, simplified local potentials, positions of branch cuts, tilted branch cuts, and state counting of PES; it includes Refs. [30–34].

[30] P. G. Harper, Single band motion of conduction electrons in a uniform magnetic field, Proc. Phys. Soc. London Sect. A **68**, 874 (1955).

[31] M. Y. Azbel, Energy spectrum of a conduction electron in a magnetic field, ZhETF, **46**, 929 (1964) [Sov. Phys. JETP **19**, 634 (1964)].

[32] D. Hofstadter, Energy levels and wave functions of Bloch electrons in rational and irrational magnetic fields, Phys. Rev. B **14**, 2239 (1976).

[33] N. Regnault and B. A. Bernevig, Fractional Chern Insulator, Phys. Rev. X **1**, 021014 (2011).

[34] G. Möller and N. R. Cooper, Fractional Chern Insulators in Harper-Hofstadter Bands with Higher Chern Number, Phys. Rev. Lett. **115**, 126401 (2015).

[35] Throughout the Letter, we keep defects well separated from each other and avoid overlaps between branch cuts and lattice sites, as detailed in Ref. [29].

[36] We assume L_x divisible by q to ensure integer number of unit cells in the x direction.

[37] M. Hafezi, P. Adhikari, and J. M. Taylor, Engineering three-body interaction and Pfaffian states in circuit QED systems, Phys. Rev. B **90**, 060503(R) (2014).

[38] Z. Liu, E. J. Bergholtz, and E. Kapit, Non-Abelian fractional Chern insulators from long-range interactions, Phys. Rev. B **88**, 205101 (2013).

[39] J. Behrmann, Z. Liu, and E. J. Bergholtz, Model Fractional Chern Insulators, Phys. Rev. Lett. **116**, 216802 (2016).

[40] X.-G. Wen and A. Zee, Shift and Spin Vector: New Topological Quantum Numbers for the Hall Fluids, Phys. Rev. Lett. **69**, 953 (1992).

[41] For a fractional quantum Hall state at filling fraction ν in the lowest Landau level on a surface of genus g, we have $N_\phi = N/\nu - \mathcal{S}_g$, where N_ϕ is the number of magnetic flux quanta penetrating the surface related to the number of single-particle states N_s in the lowest Landau level by $N_s = N_\phi + 1 - g$ [40], N is the number of particles, and $\mathcal{S}_g = \mathcal{S}_{g=0} \times (1-g)$ is the so-called topological shift [40]. For $\nu = k/2$ $\mathcal{Z}_k$ bosonic RR states, by setting $\mathcal{S}_{g=0} = 2$, we have $N_s = 2N/k - (1-g)$ as shown in Eq. (3).

[42] We pursue a good separation of scales in the many-body spectrum when we choose the locations of defects. However, we emphasize that our results are not sensitive to the precise locations of defects or the arrangement of branch cuts and crucially also hold for models including only short-range hopping once the system size is large enough [29].

[43] Taking the two-body on site interaction as an example, the interaction after projection is $H_{\mathrm{int}}^{\mathrm{proj}} = \sum_{m_1,m_2,m_3,m_4=1}^{2\phi L_x L_y + M} C_{m_1,m_2,m_3,m_4} a_{m_1}^\dagger a_{m_2}^\dagger a_{m_3} a_{m_4}$ with $C_{m_1,m_2,m_3,m_4} = \sum_{i=1}^{2L_x L_y} \psi_{m_1,i}^* \psi_{m_2,i}^* \psi_{m_3,i} \psi_{m_4,i}$, where $a_m^\dagger$ (a_m) creates (annihilates) a boson on the eigenstate ψ_m of H_0, and $\psi_m = (\psi_{m,1}, \ldots, \psi_{m,2L_xL_y})$ in the lattice site basis $a_{j,\sigma}^\dagger|\mathrm{vaccum}\rangle$.

[44] A. Sterdyniak, N. Regnault, and B. A. Bernevig, Extracting Excitations from Model State Entanglement, Phys. Rev. Lett. **106**, 100405 (2011).

[45] A. Sterdyniak, N. Regnault, and G. Möller, Particle entanglement spectra for quantum Hall states on lattices, Phys. Rev. B **86**, 165314 (2012).

[46] E. Ardonne, E. Bergholtz, J. Kailasvuori, and E. Wikberg, Degeneracy of non-Abelian quantum Hall states on the torus: domain walls and conformal field theory, J. Stat. Mech. (2008) P04016.

[47] M. Aidelsburger, M. Atala, M. Lohse, J. T. Barreiro, B. Paredes, and I. Bloch, Realization of the Hofstadter Hamiltonian with Ultracold Atoms in Optical Lattices, Phys. Rev. Lett. **111**, 185301 (2013).

[48] H. Miyake, G. A. Siviloglou, C. J. Kennedy, W. C. Burton, and W. Ketterle, Realizing the Harper Hamiltonian with Laser-Assisted Tunneling in Optical Lattices, Phys. Rev. Lett. **111**, 185302 (2013).

[49] G. Möller and N. R. Cooper, Composite Fermion Theory for Bosonic Quantum Hall States on Lattices, Phys. Rev. Lett. **103**, 105303 (2009).

[50] M. E. Tai, A. Lukin, M. Rispoli, R. Schittko, T. Menke, D. Borgnia, P. M. Preiss, F. Grusdt, A. M. Kaufman, and M. Greiner, Microscopy of the interacting Harper-Hofstadter model in the few-body limit, Nature (London) **546**, 519 (2017).

[51] P. Zupancic, P. M. Preiss, R. Ma, A. Lukin, M. E. Tai, M. Rispoli, R. Islam, and M. Greiner, Ultra-precise holographic beam shaping for microscopic quantum control, Opt. Express **24**, 13881 (2016).